

## **Associate content**

An image depicting a “48-well plate” comprising 48 individual electrochemical cells embossed in hydrophobic  $R^H$  paper; a schematic diagram showing the design and dimensions of the molds used for embossing; a representation of the technique used for the printing of electrodes; an image depicting the PDMS holder used to connect the paper-based device to a potentiostat; an analysis of the immobilization of a fluorescent antibody on the surface of  $R^H$  paper; an analysis of the electrochemical behavior of a set of independently fabricated devices in response to pAP; an analysis of the variation of the peak current potential separation with scan rate and with concentration of analyte; a discussion of the cost of fabrication per device, and a discussion of the environmental impact of disposing of devices by incineration.

Supporting Information for

**Folding Analytical Devices for Electrochemical ELISA  
in Hydrophobic R<sup>H</sup> Paper**

Ana C. Glavan<sup>1</sup>, Dionysios C. Christodouleas<sup>1</sup>, Bobak Mosadegh<sup>1</sup>, Hai Dong Yu<sup>1</sup>,  
Barbara Smith<sup>1</sup>, Joshua Lessing<sup>1</sup>, M. Teresa Fernández-Abedul<sup>1,3\*</sup> and  
George M. Whitesides<sup>1,2\*</sup>

<sup>1</sup> Department of Chemistry and Chemical Biology, Harvard University, Cambridge  
MA

<sup>2</sup> Wyss Institute for Biologically Inspired Engineering, Harvard University,  
Cambridge, MA

<sup>3</sup> Departamento de Química Física y Analítica, Universidad de Oviedo, Spain

(\*) Authors to whom correspondence should be addressed:

[gwhitesides@gmwgroup.harvard.edu](mailto:gwhitesides@gmwgroup.harvard.edu)

[mtfernandeza@uniovi.es](mailto:mtfernandeza@uniovi.es)

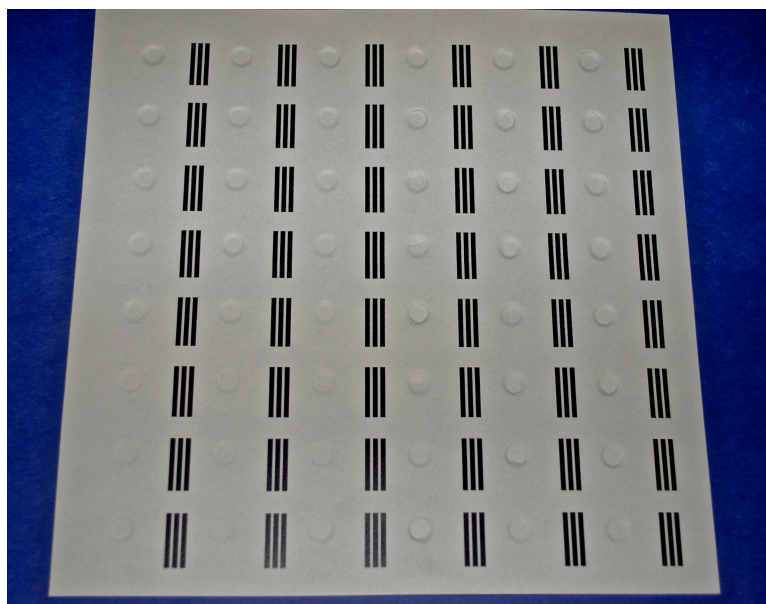


**Figure S1:** A “48 well plate” comprising 48 individual electrochemical cells. The diameter of each well is 7 mm.

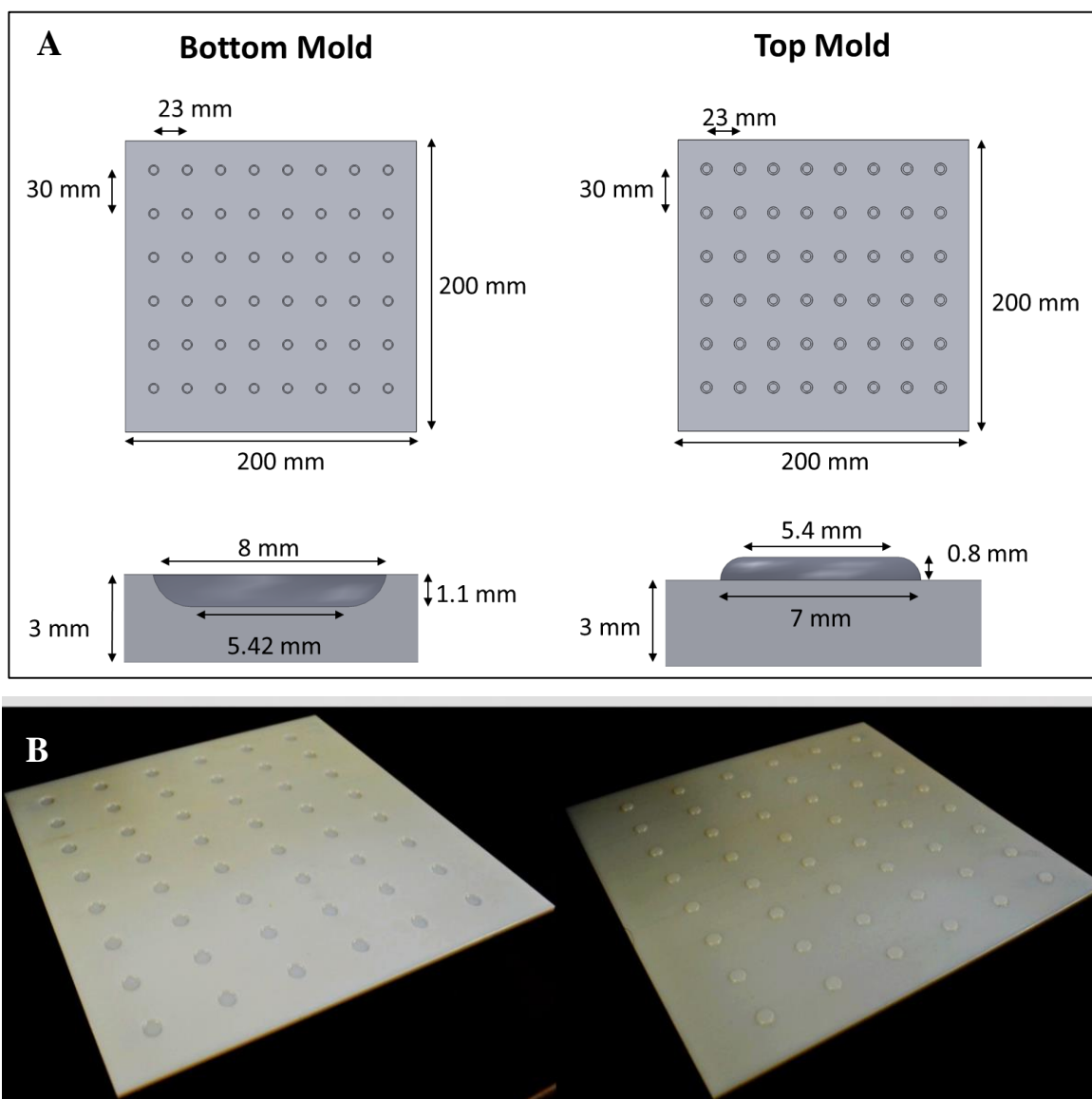


**Figure S2:** (A) Characteristic dimensions of the features in the molds used for embossing. (B) Image depicting the 200×200 mm molds used to emboss the “48 well plate”. Left: negative mold. The diameter of each feature is 8 mm; the depth of each feature is 1.1 mm. Right: positive mold. The diameter of each feature is 7 mm; the height of each feature is 0.8 mm.





**Figure S3:** Printing of electrodes using a pen filled with conductive graphite ink and a desktop cutter-plotter (Craft ROBO Cutting plotter). (A) The electrode design is loaded into ROBO Master, the software that controls the output of the plotter; B) the plotter with the paper loaded; c) the plotter prints the electrode onto the surface of the paper. The entire process takes less than 8 min for 48 electrodes.

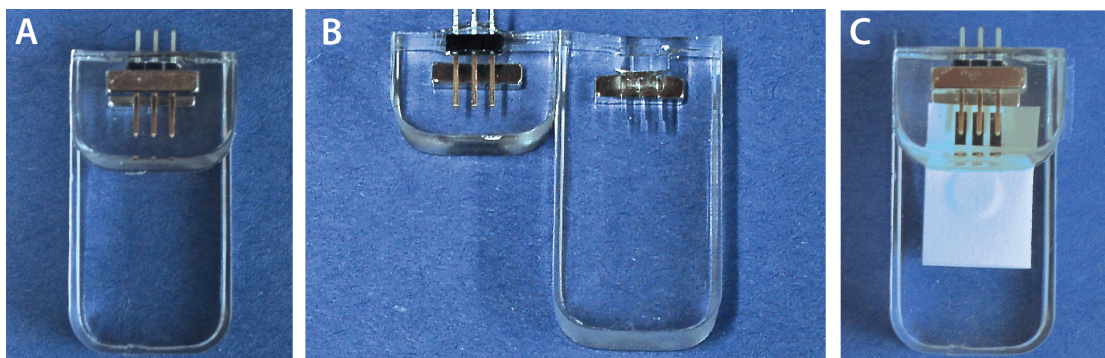


**Figure S4:** PDMS holder (A) consisting of two PDMS parts with embedded magnets (B). The holder can be used to connect the three electrodes (RE, WE and CE) of the electrochemical cell with the cable leads of a potentiostat (C).

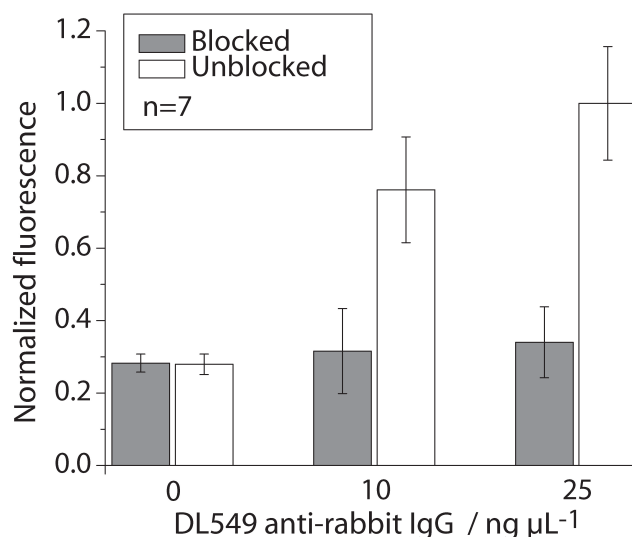


**Figure S5:** Immobilization of a fluorescent antibody (DL549 anti-rabbit IgG) on the surface of wells embossed in  $\text{C}_{10}^{\text{H}}$ -treated paper. Comparison of the fluorescence intensity from wells that were either blocked (grey bars) or unblocked (white bars) for 10 min with a solution of BSA (1% in PBS), washed, then incubated with solutions of DL549 anti-rabbit IgG (0, 10 or 25  $\text{ng } \mu\text{L}^{-1}$  in PBS, pH 7.6) for 10 min and washed. White bars indicate comparison of the fluorescence signal from wells with immobilized DL549 anti-rabbit IgG at different concentrations. The results represent the average normalized fluorescence intensity of seven independent measurements, and the error bars represent one standard deviation from the average. The results were normalized to the average fluorescence intensity of control wells (unblocked), incubated with 25  $\text{ng } \mu\text{L}^{-1}$  of antibody.

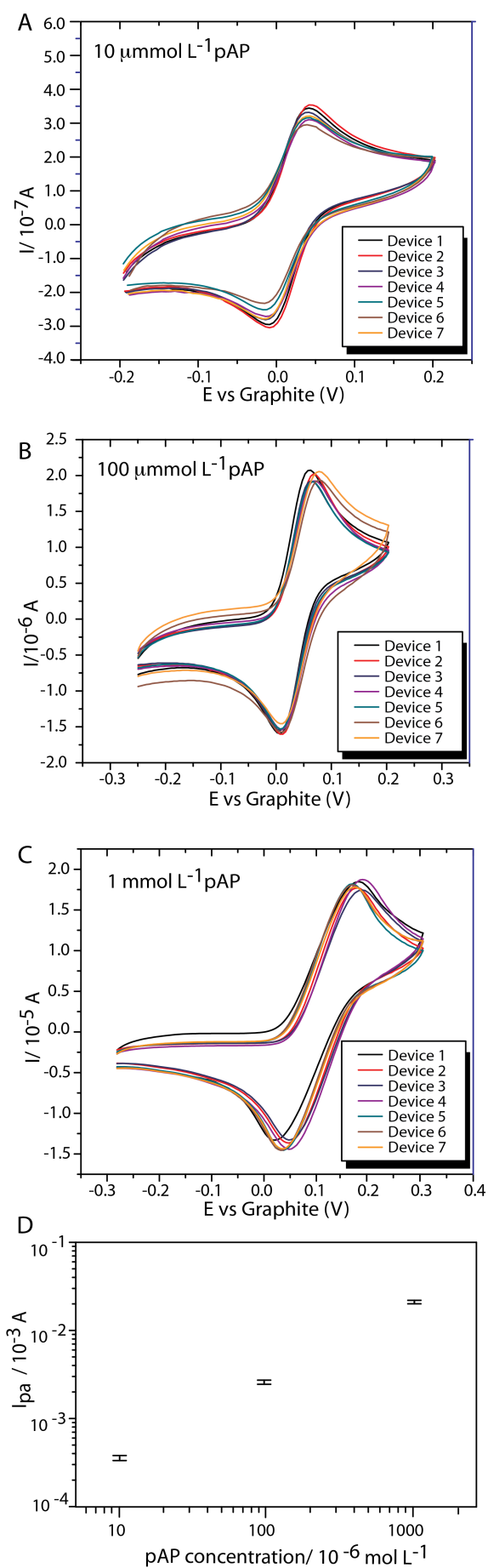


**Figure S6.** A-C) Cyclic voltammograms of pAP for a range of concentrations for seven devices prepared in different batches. D) Plot of relation between pAP concentration and measured anodic peak current (CV); the scales for both concentration and peak current are logarithmic. Each datum represents the average of seven independent measurements, and the error bars represent the standard deviation from the average.

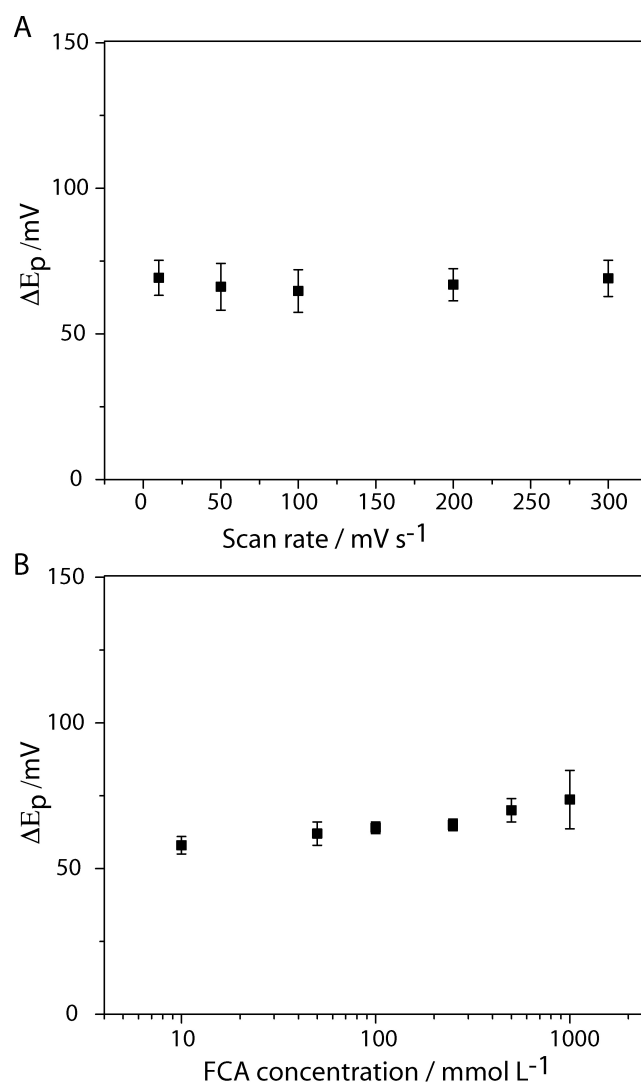


**Figure S7.** Variation of the peak current potential separation  $\Delta E_p = E_{pa} - E_{pc}$  with: (A) scan rate, for a  $100 \mu\text{mol L}^{-1}$  solution of FCA in PBS, pH 7.6; (B) concentration of FCA in PBS, pH 7.6, at a scan rate of  $100 \text{ mV s}^{-1}$ . In (B), the x-axis is logarithmic.

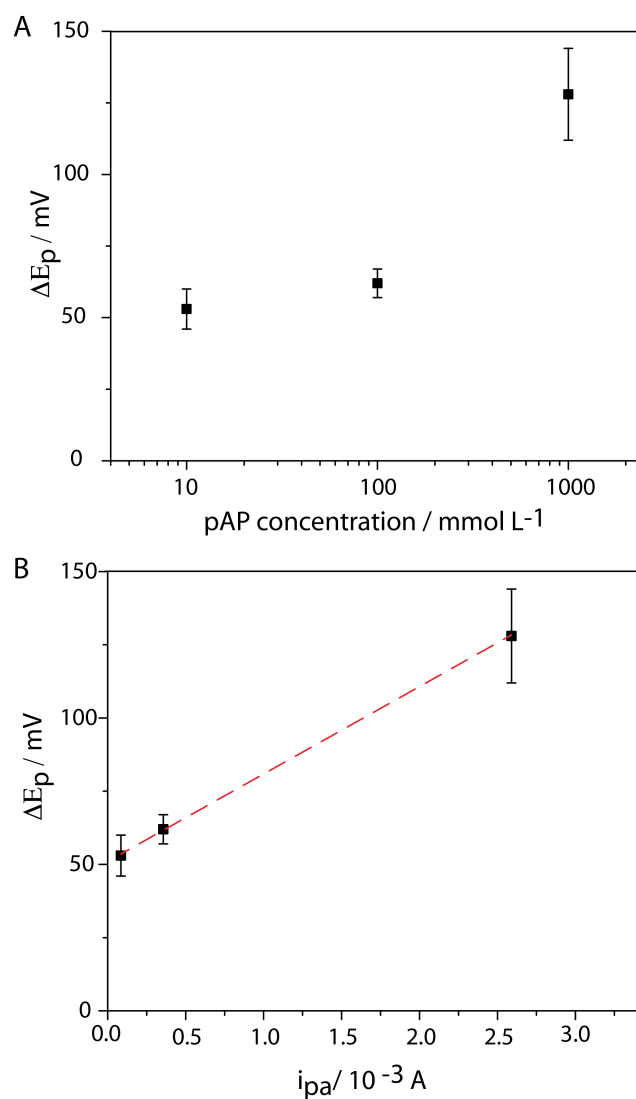


**Figure S8.** Variation of the peak current potential separation  $\Delta E_p$  with: (A) concentration, and (B) peak current measured for three concentrations of pAP [ $1 \text{ mmol L}^{-1}$ ,  $100 \text{ } \mu\text{mol L}^{-1}$ ,  $10 \text{ } \mu\text{mol L}^{-1}$ ] in PBS, pH 7.6, at a scan rate of  $100 \text{ mVs}^{-1}$ . In (A), the x-axis is logarithmic.

## **S1. Cost of Fabrication**

Excluding labor and capital expenses, we estimate the cost for making any of the microfluidic devices described in this paper be less than \$0.007 (all prices are for small or research quantities of materials and reagents): i) The estimated cost of the paper is less than \$0.004 ( $\sim 6 \text{ cm}^2$  at \$0.0007 per  $\text{cm}^2$  for Whatman Chr 1 chromatography paper). ii) The estimated cost of the organosilane is less than \$0.00008 per  $\text{cm}^2$  ( $\sim \$1$  per gram; we estimate that 40  $\mu\text{L}$  of organosilane can functionalize over one hundred  $6 \text{ cm}^2$  devices). iii) The estimated cost of the graphite ink (Gwent graphite paste diluted in Ercon N-160 solvent thinner) is less than \$0.001 per device.

Cost considerations. Broken down into 3 categories: materials (cost per device), fabrication (cost of machinery), and packaging (cost per device).



**Table S1. Cost of fabrication per device**

<b>Item</b>	<b>Used per device</b>	<b>Cost</b>	<b>Total cost per device</b>
<b>Whatman Chr 1 paper</b>	6 cm <sup>2</sup>	\$0.52 / 400 cm <sup>2</sup> sheet	\$0.0040
<b>Organosilane</b>	< 1μL	\$1.00 / gram	\$0.0001
<b>Gwent graphite paste in solvent</b>	20 mg	\$0.20 /gram	\$0.0010
<b>Graphtec Craft Robo Pro</b>	1 machine	\$1,200.00	< \$0.0001
<b>Ink pen with refillable cartridge</b>	1 pen	\$10.00	< \$0.0001
<b>Cutting platform</b>	1 package of 3	\$15.00	< \$0.0001
<b>Technician</b>	1 worker	\$30,000.00/year	< \$0.0001
<b>Total cost per device</b>			~\$0.0060

## S2. Device Disposal by burning

The organosilane used to functionalize the paper is not fluorinated. Paper functionalized with decyl trichlorosilane can be burned without significant environmental consequences in order to dispose of potentially contaminated samples.

## S3. Variation of the peak current potential separation $\Delta E_p$ with concentration

To distinguish between kinetic and resistive effects in the solution of pAP, we have plotted the peak potential separation versus peak current for different concentrations of analyte at a potential scan rate of 100 mV s<sup>-1</sup> (Figure S8). The measured cathodic-to-anodic peak potential separation,  $\Delta E_p$  (V), and the ohmic resistance in the cell,  $R$  ( $\Omega$ ), are related by the following equation:<sup>1</sup>

$$\Delta E_p = (\Delta E_p)_{kin} + 2i_p R \quad Eq. 1$$

The ordinate at the origin in this equation,  $(\Delta E_p)_{kin}$  (V), is related to kinetic parameters of the interfacial electron transfer process.<sup>2</sup>

For pAP, we plotted  $\Delta E_p$  vs  $i_p$ , and used a simple linear regression to test the linearity of the two variables. The data fit the linear regression  $y=a + bx$ , with  $R^2=0.998$ ,  $a=0.051$  V, and  $b=29.86$   $\Omega$ ; thus,  $R \sim 15$   $\Omega$ .

Since the resistance in the cell is not high ( $< 100$   $\Omega$ ), we hypothesize that the shift in cathodic-to-anodic peak potential separation is caused by slow or quasi-reversible electron-transfer kinetics from pAP to the electrode surface. pAP has been found to be quasi-reversible in other electrochemical systems.<sup>3</sup> In addition, the shift in cathodic-to-anodic peak potential separation is not significant in the CV of a molecule with fast electron transfer kinetics, FCA, at the same concentration (1 mmol L<sup>-1</sup>), electrolyte solution and scan rate, which should exhibit comparable uncompensated solution resistance (see Figure S7).

## References:

- (1) Carbó, A. D. *Electrochemistry of porous materials*; CRC press, 2010, p.15-18.
- (2) Nicholson, R. S. *Anal. Chem.* **1965**, 37, 1351-1355.
- (3) Mehretie, S.; Admassie, S.; Hunde, T.; Tessema, M.; Solomon, T. *Talanta* **2011**, 85, 1376-1382.